

Search for Doubly-Charged Higgs Bosons at LEP

The L3 Collaboration

Abstract

Doubly-charged Higgs bosons are searched for in e^+e^- collision data collected with the L3 detector at LEP at centre-of-mass energies up to 209 GeV. Final states with four leptons are analysed to tag the pair-production of doubly-charged Higgs bosons. No significant excess is found and lower limits at 95% confidence level on the doubly charged Higgs boson mass are derived. They vary from 95.5 GeV to 100.2 GeV, depending on the decay mode. Doubly-charged Higgs bosons which couple to electrons would modify the cross section and forward-backward asymmetry of the $e^+e^- \rightarrow e^+e^-$ process. The measurements of these quantities do not deviate from the Standard Model expectations and doubly-charged Higgs bosons with masses up to the order of a TeV are excluded.

Submitted to *Phys. Lett. B*

Introduction

In the Standard Model of the electroweak interactions [1] the masses of the fermions and bosons are explained by the Higgs mechanism [2]. A consequence of this mechanism is the existence of an additional particle, the Higgs boson, which, to date, has not been directly observed [3, 4]. Extensions of the Standard Model predict additional Higgs bosons which can be lighter and hence accessible at current experimental facilities. Among these, doubly-charged Higgs bosons, $H^{\pm\pm}$, are expected [5] in several scenarios such as Higgs triplet models, left-right symmetric models and, recently, little Higgs models [6].

Doubly-charged Higgs bosons can be light enough [7] to be directly accessible in e^+e^- collisions at LEP through the pair-production mechanism, depicted in Figures 1a and 1b. In addition, they can contribute to $e^+e^- \rightarrow e^+e^-$ scattering as sketched in Figure 1c, producing measurable deviations in the cross section and forward-backward asymmetries for masses of the order of a TeV. This Letter describes the direct search for pair-produced doubly-charged Higgs bosons and the constraints derived from the precision measurement of the $e^+e^- \rightarrow e^+e^-$ scattering. Data collected with the L3 detector [7] at centre-of-mass energies, \sqrt{s} , up to 209 GeV are used. Results from other LEP experiments were recently reported [9].

The $H^{\pm\pm}$ couplings to charged leptons are parametrised by the parameters $h_{\ell\ell'}$, where ℓ and ℓ' denote the charged lepton flavour. The search for pair-produced doubly-charged Higgs bosons described below assumes $h_{\ell\ell'} > 10^{-7}$ to ensure that the $H^{\pm\pm}$ decays before entering the detector and $h_{e\ell} < 10^{-3}$ to suppress large contributions to the cross section from the t -channel diagram of Figure 1b. The latter assumption corresponds to a conservative estimate of the experimental sensitivities.

Doubly-charged Higgs bosons are conventionally labeled as “left-handed” or “right-handed” [5], referring to different couplings rather than different helicities. Left-handed $H^{\pm\pm}$ couple to the Z boson and the additional s -channel diagram results in a pair-production cross section larger than for right-handed $H^{\pm\pm}$. The analysis discussed below concentrates on the latter, less favourable, case. The cross section for the $e^+e^- \rightarrow H^{++}H^{--}$ process depends [10, 11] only on the mass of the doubly-charged Higgs boson, m_H , and on \sqrt{s} . For $\sqrt{s} = 206$ GeV, it varies from 1 pb for $m_H = 60$ GeV down to 0.1 pb for $m_H = 95$ GeV.

Pair-production of doubly-charged Higgs bosons produces events with four charged leptons whose flavour depends on the $h_{\ell\ell'}$ coupling. In the following, all six possible couplings are considered: h_{ee} , $h_{e\mu}$, $h_{e\tau}$, $h_{\mu\mu}$, $h_{\mu\tau}$ and $h_{\tau\tau}$, with the hypothesis that only one coupling at a time is different from zero, which implies that both doubly-charged Higgs bosons in the events have the same decay mode.

If the doubly-charged Higgs boson couples to electrons, it contributes to the differential cross section of the $e^+e^- \rightarrow e^+e^-$ process through interference with the additional u -channel Feynman diagram depicted in Figure 1c. This additional term is calculated [10] to be proportional to

$$\frac{h_{ee}^2}{m_H^2 - u}$$

where $u = -s(1 + \cos\theta)/2$ and θ is the electron scattering angle. In the following, information on h_{ee} and m_H is extracted from the comparison of the measured cross section and the forward-backward asymmetry of the $e^+e^- \rightarrow e^+e^-$ process with the Standard Model predictions and the doubly charged Higgs contribution.

Data and Monte Carlo Samples

The search for pair-produced $H^{\pm\pm}$ uses 624.1 pb^{-1} of data collected at $\sqrt{s} = 189 - 209 \text{ GeV}$. Table 1 details the average \sqrt{s} values for the different data taking periods and the corresponding integrated luminosities. Constraints on $H^{\pm\pm}$ contributions to the $e^+e^- \rightarrow e^+e^-$ process are derived from these data and from an additional 66.4 pb^{-1} collected at $\sqrt{s} = 130 - 183 \text{ GeV}$.

For the optimisation of the selection and efficiency studies, Monte Carlo events of the process $e^+e^- \rightarrow H^{++}H^{--} \rightarrow \ell^+\ell'^+\ell^-\ell'^-$ are generated according to the differential cross sections of References 10 and 11. Effects of initial state radiation are included [12] in the generation and final state radiation is modelled with the PHOTOS [13] Monte Carlo. For each \sqrt{s} value listed in Table 1, several m_H points are considered: $m_H = 45 \text{ GeV}$ and from $m_H = 65 \text{ GeV}$ up to the kinematic limit $\sqrt{s}/2$, in steps of 5 GeV . For each m_H point, 5000 events are generated for each of the six $h_{\ell\ell'}$ couplings. Decays of the tau leptons are described with the TAUOLA [14] Monte Carlo program and JETSET [15] is used to model hadrons produced in these decays.

Standard Model processes are modelled with the following Monte Carlo generators: KK2f [16] for $e^+e^- \rightarrow q\bar{q}(\gamma)$, $e^+e^- \rightarrow \mu^+\mu^-(\gamma)$ and $e^+e^- \rightarrow \tau^+\tau^-(\gamma)$, BHWIDE [17] for $e^+e^- \rightarrow e^+e^-(\gamma)$, EXCALIBUR [18] for the four-fermion processes $e^+e^- \rightarrow q\bar{q}'e\nu_e$, $e^+e^- \rightarrow \ell^+\ell^-q\bar{q}$ and $e^+e^- \rightarrow \ell^+\ell^-\ell'^+\ell'^-$, PYTHIA [15] and KORALW [19] for four-fermion final states of the $e^+e^- \rightarrow ZZ$ and $e^+e^- \rightarrow W^+W^-$ processes, respectively, which are not covered by the EXCALIBUR simulations and PHOJET [20] and DIAG36 [21] for hadron and lepton production in two-photon interactions, respectively. The L3 detector response is simulated using the GEANT program [22] which takes into account the effects of energy loss, multiple scattering and showering in the detector. Time-dependent detector inefficiencies, as monitored during the data taking periods, are included in the simulations.

Search for Pair-Produced Doubly-Charged Higgs Bosons

The signature of the $e^+e^- \rightarrow H^{++}H^{--} \rightarrow \ell^+\ell'^+\ell^-\ell'^-$ process consists of four leptons, whose flavour depends on the $h_{\ell\ell'}$ coupling. For electrons, muons or leptonically decaying tau leptons this signature is clean and little background is expected from lepton pair-production and four-fermion processes. Events with tau leptons which decay into hadrons have a larger background from the four-fermion $e^+e^- \rightarrow \ell^+\ell^-q\bar{q}$ process and from two-photon interactions. The analysis proceeds from the identification of leptons to the preselection of events compatible with the signal signature. Finally, cuts on the lepton energies and global event variables further reduce backgrounds.

Electrons are identified by requiring a well isolated cluster in the electromagnetic calorimeter, formed by at least two adjacent crystals, with an associated track in the tracking chamber. The shower shape of this cluster must be compatible with that of an electromagnetic particle.

Muons are reconstructed by requiring tracks in the muon spectrometer matched with tracks in the central tracker. To reject cosmic background, muon candidates must be in time with the beam crossing.

In addition to their leptonic decays, tau leptons are identified by requiring low-multiplicity jets associated with one, two or three tracks. Narrow and isolated jets are selected by comparing their energy to that deposited in 10° and 30° cones around the jet axes.

To increase the selection efficiency, two additional classes of particles are considered: photons, which correspond to electron candidates which fail the track matching criteria, and minimum ionising particles in the calorimeters, MIPs, having an associated track in the central

tracker, which tag muons.

Nine analyses are built which rely on the exclusive identification of four leptons. They are denoted as: $eeee$, $eee\gamma$, $ee\mu\mu$, $e\gamma\mu\mu$, $ee\tau\tau$, $\mu\mu\mu\mu$, $\mu\mu\mu$ MIP, $\mu\mu\tau\tau$, and $\tau\tau\tau\tau$. Each analysis is used in the study of one or more $h_{\ell\ell'}$ couplings, as summarised in Table 2.

In addition, three semi-inclusive selections are devised to increase the selection efficiency for final states with tau leptons decaying into hadrons. These selections first identify an electron or a muon pair in hadronic events, including the case in which one of the electrons is tagged as a photon, and then force the remaining particles of the event into two jets by means of the DURHAM [23] algorithm. These two jets are considered as tau lepton candidates. The selections are denoted as: ee jetjet, $e\gamma$ jetjet and $\mu\mu$ jetjet. They are used for the analyses of the $h_{e\tau}$, $h_{\mu\tau}$ and $h_{\tau\tau}$ couplings, as detailed in Table 2.

Event Selection

Low-multiplicity events with more than three but less than ten tracks and visible energy in excess of $0.3\sqrt{s}$ are selected. Two classes of events are accepted: events with at least three particles identified as electrons, muons or tau leptons or events with two jets and an electron or muon pair or one electron and one photon. The numbers of events obtained by this preselection are given in Table 3, where the results of the twelve different analyses are combined and presented for the six $h_{\ell\ell'}$ couplings. Good agreement is observed between data and Standard Model expectations.

Several discriminating variables are considered to increase the sensitivity of the analysis.

- The energy of the most energetic lepton, E_1 , is close to $0.5\sqrt{s}$ for the background from two-fermion events, and peaks around $0.25\sqrt{s}$ for the signal, which predicts a similar energy sharing for all leptons of the event. A cut around $E_1 < 0.45\sqrt{s}$ is used by all twelve selections. As an example, the distributions for the $eee\gamma$ analysis are shown in Figure 2a.
- The energy of the second most energetic lepton tends to be high for background events and peaked around $0.25\sqrt{s}$ for the signal. A cut around $0.35\sqrt{s}$ is applied for the ee jetjet and $\mu\mu$ jetjet analyses.
- The energy of the selected photon, E_γ , for initial state radiation photons from fermion pair-production has a high energy tail, as shown in Figure 2b for the $e\gamma$ jetjet selection. A cut around $E_\gamma < 0.3\sqrt{s}$ is applied for all analyses which accept photons. For events of the $eee\gamma$ and $e\gamma\mu\mu$ analyses, an additional cut around $E_\gamma > 0.2\sqrt{s}$ is applied, to enforce the signal topology which predicts lepton energies around $0.25\sqrt{s}$.
- The energy of the third most energetic lepton, E_3 , is low for the background from two-fermion processes and non-resonant or single-resonant four-fermion production and also peaks around $0.25\sqrt{s}$ for the signal. A cut around $E_3 > 0.1\sqrt{s}$ is applied for the $ee\mu\mu$ selection, whose distributions are shown in Figure 2c.
- Events with jets in the final state suffer from a potentially large background from two-photon processes. This is reduced by requiring that an energy less than 30 GeV is deposited in the calorimeters in a 30° angle around the beam line and the projection of the missing momentum vector on this direction is less than 50 GeV. The presence of neutrinos

in tau lepton decays gives signal events a momentum imbalance in the plane transverse to the beam axis, P_t , as shown in Figure 2d for the ee jet jet analysis. A cut $P_t > 5$ GeV is applied, further reducing events from fermion pair-production and two-photon processes which have small values of P_t .

The twelve selections listed in Table 2 are simultaneously applied and their yields are combined for the six couplings. The nine selections without jets in the final state are largely complementary, while a large overlap is observed between the ee jet jet and $ee\tau\tau$ selections. Additional selections like $ee\gamma\gamma$ and μ MIP jet jet are found not to increase the signal sensitivity.

Results and Interpretation

Table 3 compares the number of events observed after final selection with the Standard Model expectations. Good agreement is observed and no evidence is found for a signal due to doubly-charged Higgs bosons. The number of expected signal events for $m_H = 95$ GeV and the selection efficiencies for the range $m_H = 60 - 100$ GeV are also given.

The sensitivity of the analysis is enhanced by the reconstruction of the mass of the candidate Higgs bosons. For each coupling, all pairings of leptons with a flavour consistent with doubly-charged Higgs boson decay are considered and their invariant and recoil masses are calculated. The pairing with the smallest difference between these two masses is retained and their average is used as an estimate of m_H . The distributions of the reconstructed mass for data, Standard Model and signal Monte Carlo are presented in Figure 3. No structure possibly due to a doubly-charged Higgs signal is observed.

In the absence of a signal, upper limits on the production cross section of doubly-charged Higgs bosons are derived as a function of m_H and converted to lower limits on m_H . The log-likelihood ratio technique [4] is used to calculate the observed and expected 95% confidence level cross section limits, presented, as a function of m_H for the different couplings, in Figures 4 and 5. Cross sections between 0.1 pb and 0.01 pb are excluded, depending on m_H and on the coupling.

The limits include systematic uncertainties on the signal efficiency and the background normalisation. These follow from uncertainties in the determination of the energy scale of the detector, on the event selection and lepton identification criteria, on Monte Carlo statistics and on the cross section of the Standard Model background processes. Table 4 gives the total systematic uncertainties for the different couplings. These uncertainties reduce the sensitivity by a few hundred MeV.

Lower limits on m_H are extracted by comparing the cross section upper limits with the known cross section of the process $e^+e^- \rightarrow H^{++}H^{--}$ [10,11]. The most conservative scenario of a right-handed $H^{\pm\pm}$ and the absence of a t -channel contribution to $H^{\pm\pm}$ production is considered. The observed limits vary from 95.5 GeV to 100.2 GeV, depending on the coupling and are listed in Table 5 together with the expected ones.

Constraints from Bhabha Scattering

The measurements of the cross sections and forward-backward asymmetries of the $e^+e^- \rightarrow e^+e^-$ process in 243.7 pb^{-1} of data at $\sqrt{s} = 130 - 189$ GeV are described in Reference 24 and found to be in good agreement with the Standard Model predictions [25,26]. Similar analyses are applied to 446.8 pb^{-1} of data collected at $\sqrt{s} = 192 - 209$ GeV. The results are also in good

agreement with the Standard Model predictions, and show no evidence for the exchange of a doubly-charged Higgs boson.

A fit for h_{ee} is performed to the measured cross sections and forward-backward asymmetries for $\sqrt{s} = 130 - 209$ GeV and several hypotheses on the value of m_H . Experimental systematic uncertainties [24] and uncertainties on the Standard Model predictions [27] are taken into account in the fit. Upper limits on h_{ee} at 95% confidence level are derived as a function of m_H and shown in Figure 6. The exclusion region for $h_{ee} > 0.7$ extends to the TeV scale and is complementary to that derived here from the search for pair-production of doubly-charged Higgs bosons.

References

- [1] S.L. Glashow, Nucl. Phys. **22** (1961) 579; S. Weinberg, Phys. Rev. Lett. **19** (1967) 1264; A. Salam, *Elementary Particle Theory*, edited by N. Svartholm (Almqvist and Wiksell, Stockholm, 1968), p. 367
- [2] P.W. Higgs, Phys. Lett. **12** (1964) 132, Phys. Rev. Lett. **13** (1964) 508; Phys. Rev. **145** (1966) 1156; F. Englert and R. Brout, Phys. Rev. Lett. **13** (1964) 321; G.S. Guralnik, C.R. Hagen and T.W.B. Kibble, Phys. Rev. Lett. **13** (1964) 585
- [3] L3 Collab. P. Achard *et al.*, Phys. Lett. **B 517** (2001) 319
- [4] ALEPH, DELPHI, L3 and OPAL Collab., The LEP Working Group for Higgs Boson Searches, Phys. Lett. **B 565** (2003) 61
- [5] R.N. Mohapatra and J.D. Vergados, Phys. Rev. Lett. **47** (1981) 1713; G.B. Gelmini and M. Roncadelli, Phys. Lett. **B 99** (1981) 411; V.D. Barger *et al.*, Phys. Rev. **D 26** (1982) 218; T. Rizzo, Phys. Rev. **D 25** (1982) 1355; M. Lusignoli and S. Petrarca, Phys. Lett. **B 226** (1989) 397; J.F. Gunion, Int. J. Mod. Phys. **A 11** (1996) 1551; R.N. Mohapatra and G. Senjanovic, Phys. Rev. **D 23** (1981) 165
- [6] N. Arkani-Hamed, A.G. Cohen and H. Georgi, Phys. Lett. **B 513** (2001) 232; N. Arkani-Hamed *et al.*, JHEP **0208** (2002) 020; N. Arkani-Hamed *et al.*, JHEP **0208** (2002) 021; T. Han *et al.*, Phys. Rev. **D 67** (2003) 0905004
- [7] C.S. Aulakh *et al.*, Phys. Rev. **D 57** (1998) 4174; Z. Chacko and R.N. Mohapatra, Phys. Rev. **D 58** (1998) 015003; B. Dutta and R.N. Mohapatra, Phys. Rev. **D 59** (1999) 015018
- [8] L3 Collab., B. Adeva *et al.*, Nucl. Inst. Meth. **A 289** (1990) 35; L3 Collab., O. Adriani *et al.*, Phys. Rept. **236** (1993) 1; M. Chemarin *et al.*, Nucl. Inst. Meth. **A 349** (1994) 345; G. Basti *et al.*, Nucl. Inst. Meth. **A 374** (1996) 293; A. Adam *et al.*, Nucl. Inst. Meth. **A 383** (1996) 342; I.C. Brock *et al.*, Nucl. Instr. and Meth. **A 381** (1996) 236; M. Acciarri *et al.*, Nucl. Inst. Meth. **A 351** (1994) 300
- [9] OPAL Collab. G. Abbiendi *et al.*, Phys. Lett. **B 526** (2002) 221; DELPHI Collab. J. Abdallah *et al.*, Phys. Lett. **B 552** (2003) 127; OPAL Collab. G. Abbiendi *et al.*, Preprint hep-ex/0308052 (2003)
- [10] M.L. Swartz, Phys. Rev. **D 40** (1989) 1521

- [11] K. Huitu *et al.*, Helsinki Institute of Physics Report HIP-1998-06 (1998)
- [12] F.A. Berends and R. Kleiss, Nucl. Phys. **B 260** (1985) 32
- [13] PHOTOS version 2.0 is used; E. Barberio and Z. Wąs, Comp. Phys. Comm. **79** (1994) 291
- [14] TAUOLA version 2.4 is used; S. Jadach *et al.*, Comp. Phys. Comm. **76** (1993) 361
- [15] JETSET version 7.3 and PYTHIA version 5.722 are used; T. Sjöstrand, preprint CERN-TH/7112/93 (1993), revised 1995; Comp. Phys. Comm. **82** (1994) 74
- [16] KK2f version 4.14 is used; S. Jadach, B.F.L. Ward and Z. Wąs, Comp. Phys. Comm **130** (2000) 260
- [17] BHWIDE version 1.03 is used; S. Jadach, W. Placzek and B.F.L. Ward, Phys. Lett. **B 390** (1997) 298
- [18] EXCALIBUR version 1.11 is used; F.A. Berends, R. Kleiss and R. Pittau, Comp. Phys. Comm. **85** (1995) 437
- [19] KORALW version 1.33 is used; M. Skrzypek *et al.*, Comp. Phys. Comm. **94** (1996) 216; M. Skrzypek *et al.*, Phys. Lett. **B 372** (1996) 289
- [20] PHOJET version 1.05 is used; R. Engel, Z. Phys. **C 66** (1995) 203; R. Engel and J. Ranft, Phys. Rev. **D 54** (1996) 4244
- [21] DIAG 36 Monte Carlo; F.A. Berends, P.H. Daverfeldt and R. Kleiss, Nucl. Phys. **B 253** (1985) 441
- [22] GEANT version 3.15 is used; R. Brun *et al.*, preprint CERN DD/EE/84-1 (1985), revised 1987. The GHEISHA program (H. Fesefeldt, RWTH Aachen Report PITHA 85/02, 1985) is used to simulate hadronic interactions
- [23] S. Bethke *et al.*, Nucl. Phys. **B 370** (1992) 310
- [24] L3 Collab. M. Acciarri *et al.*, Phys. Lett. **B 479** (2000) 101
- [25] ZFITTER version 6.21 is used; D. Bardin *et al.*, Comp. Phys. Comm. **133** (2001) 229
- [26] TOPAZ0 version 4.4 is used; G. Montagna *et al.*, Comp. Phys. Comm. **76** (1993) 328
- [27] M. Kobel *et al.*, CERN Report 2000-009, Preprint hep-ph/0007180 (2000).

Author List

The L3 Collaboration:

P.Achard²⁰ O.Adriani¹⁷ M.Aguilar-Benitez²⁴ J.Alcaraz²⁴ G.Alemanni²² J.Allaby¹⁸ A.Aloisio²⁸ M.G.Alvigi²⁸
H.Anderhub⁴⁶ V.P.Andreev^{6,33} F.Anselmo⁸ A.Arefiev²⁷ T.Azmoon³ T.Aziz⁹ P.Bagnaia³⁸ A.Bajo²⁴ G.Baksay²⁵
L.Baksay²⁵ S.V.Baldew² S.Banerjee⁹ Sw.Banerjee⁴ A.Barczyk^{46,44} R.Barillère¹⁸ P.Bartalini²² M.Basile⁸
N.Batalova⁴³ R.Battiston³² A.Bay²² F.Becattini¹⁷ U.Becker¹³ F.Behner⁴⁶ L.Bellucci¹⁷ R.Berbeco³ J.Berdugo²⁴
P.Berges¹³ B.Bertucci³² B.L.Betev⁴⁶ M.Biasini³² M.Biglietti²⁸ A.Biland⁴⁶ J.J.Blaising⁴ S.C.Blyth³⁴
G.J.Bobbink² A.Böhm¹ L.Boldizsar¹² B.Borgia³⁸ S.Bottai¹⁷ D.Bourilkov⁴⁶ M.Bourquin²⁰ S.Braccini²⁰
J.G.Branson⁴⁰ F.Brochu⁴ J.D.Burger¹³ W.J.Burger³² X.D.Cai¹³ M.Capell¹³ G.Cara Romeo⁸ G.Carlino²⁸
A.Cartacci¹⁷ J.Casaus²⁴ F.Cavallari³⁸ N.Cavallo³⁵ C.Cecchi³² M.Cerrada²⁴ M.Chamizo²⁰ Y.H.Chang⁴⁸
M.Chemarin²³ A.Chen⁴⁸ G.Chen⁷ G.M.Chen⁷ H.F.Chen²¹ H.S.Chen⁷ G.Chiefari²⁸ L.Cifarelli³⁹ F.Cindolo⁸
I.Clare¹³ R.Clare³⁷ G.Coignet⁴ N.Colino²⁴ S.Costantini³⁸ B.de la Cruz²⁴ S.Cucciarelli³² J.A.van Dalen³⁰
R.de Asmundis²⁸ P.Déglon²⁰ J.Debreczeni¹² A.Degré⁴ K.Dehmelt²⁵ K.Deiters⁴⁴ D.della Volpe²⁸ E.Delmeire²⁰
P.Denes³⁶ F.DeNotaristefani³⁸ A.De Salvo⁴⁶ M.Diemoz³⁸ M.Dierckxsens² C.Dionisi³⁸ M.Dittmar⁴⁶ A.Doria²⁸
M.T.Dova^{10,4} D.Duchesneau⁴ M.Duda¹ B.Echenard²⁰ A.Eline¹⁸ A.El Hage¹ H.El Mamouni²³ A.Engler³⁴
F.J.Eppling¹³ P.Extermann²⁰ M.A.Falagan²⁴ S.Falciano³⁸ A.Favara³¹ J.Fay²³ O.Fedin³³ M.Felcini⁴⁶ T.Ferguson³⁴
H.Fesefeldt¹ E.Fiandrini³² J.H.Field²⁰ F.Filthaut³⁰ P.H.Fisher¹³ W.Fisher³⁶ I.Fisk⁴⁰ G.Forconi¹³
K.Freudenreich⁴⁶ C.Furetta²⁶ Yu.Galaktionov^{27,13} S.N.Ganguli⁹ P.Garcia-Abia²⁴ M.Gataullin³¹ S.Gentile³⁸
S.Giagu³⁸ Z.F.Gong²¹ F.Greco²⁸ G.Grenier²³ O.Grimm⁴⁶ M.W.Gruenewald¹⁶ M.Guida³⁹ R.van Gulik²
V.K.Gupta³⁶ A.Gurtu⁹ L.J.Gutay⁴³ D.Haas⁵ D.Hatzifotiadou⁸ T.Hebbeker¹ A.Hervé¹⁸ J.Hirschfelder³⁴
H.Hofer⁴⁶ M.Hohlmann²⁵ G.Holzner⁴⁶ S.R.Hou⁴⁸ Y.Hu³⁰ B.N.Jin⁷ L.W.Jones³ P.de Jong² I.Josa-Mutuberría²⁴
D.Käfer¹ M.Kaur¹⁴ M.N.Kienzle-Focacci²⁰ J.K.Kim⁴² J.Kirkby¹⁸ W.Kittel³⁰ A.Klimentov^{13,27} A.C.König³⁰
M.Kopal⁴³ V.Koutsenko^{13,27} M.Kräber⁴⁶ R.W.Kraemer³⁴ A.Krüger⁴⁵ A.Kunin¹³ P.Ladron de Guevara²⁴
I.Laktineh²³ G.Landi¹⁷ M.Lebeau¹⁸ A.Lebedev¹³ P.Lebrun²³ P.Lecomte⁴⁶ P.Lecoq¹⁸ P.Le Coultre⁴⁶
J.M.Le Goff¹⁸ R.Leiste⁴⁵ M.Levtchenko²⁶ P.Levtchenko³³ C.Li²¹ S.Likhoded⁴⁵ C.H.Lin⁴⁸ W.T.Lin⁴⁸ F.L.Linde²
L.Lista²⁸ Z.A.Liu⁷ W.Lohmann⁴⁵ E.Longo³⁸ Y.S.Lu⁷ C.Luci³⁸ L.Luminari³⁸ W.Lustermann⁴⁶ W.G.Ma²¹
L.Malgeri²⁰ A.Malinin²⁷ C.Mañá²⁴ J.Mans³⁶ J.P.Martin²³ F.Marzano³⁸ K.Mazumdar⁹ R.R.McNeil⁶ S.Mele^{18,28}
L.Merola²⁸ M.Meschini¹⁷ W.J.Metzger³⁰ A.Mihul¹¹ H.Milcent¹⁸ G.Mirabelli³⁸ J.Mnich¹ G.B.Mohanty⁹
G.S.Muanza²³ A.J.M.Muijs² B.Musicar⁴⁰ M.Musy³⁸ S.Nagy¹⁵ S.Natale²⁰ M.Napolitano²⁸ F.Nessi-Tedaldi⁴⁶
H.Newman³¹ A.Nisati³⁸ T.Novak³⁰ H.Nowak⁴⁵ R.Ofierzynski⁴⁶ G.Organtini³⁸ I.Pal⁴³ C.Palomares²⁴ P.Paolucci²⁸
R.Paramatti³⁸ G.Passaleva¹⁷ S.Patricelli²⁸ T.Paul¹⁰ M.Pauluzzi³² C.Paus¹³ F.Pauss⁴⁶ M.Pedace³⁸ S.Pensotti²⁶
D.Perret-Gallix⁴ B.Petersen³⁰ D.Piccolo²⁸ F.Pierella⁸ M.Pioppi³² P.A.Piroué³⁶ E.Pistoletti²⁶ V.Plyaskin²⁷
M.Pohl²⁰ V.Pojidaev¹⁷ J.Pothier¹⁸ D.Prokofiev³³ J.Quartier³⁹ G.Rahal-Callot⁴⁶ M.A.Rahaman⁹ P.Raics¹⁵
N.Raja⁹ R.Ramelli⁴⁶ P.G.Rancoita²⁶ R.Ranieri¹⁷ A.Raspereza⁴⁵ P.Razis²⁹ D.Ren⁴⁶ M.Rescigno³⁸ S.Reucroft¹⁰
S.Riemann⁴⁵ K.Riles³ B.P.Roe³ L.Romero²⁴ A.Rosca⁴⁵ C.Rosenbleck¹ S.Rosier-Lees⁴ S.Roth¹ J.A.Rubio¹⁸
G.Ruggiero¹⁷ H.Rykaczewski⁴⁶ A.Sakharov⁴⁶ S.Saremi⁶ S.Sarkar³⁸ J.Salicio¹⁸ E.Sanchez²⁴ C.Schäfer¹⁸
V.Schegelsky³³ H.Schopper⁴⁷ D.J.Schotanus³⁰ C.Sciacca²⁸ L.Servoli³² S.Shevchenko³¹ N.Shivarov⁴¹ V.Shoutko¹³
E.Shumilov²⁷ A.Shvorob³¹ D.Son⁴² C.Souga²³ P.Spillantini¹⁷ M.Steuer¹³ D.P.Stickland³⁶ B.Stoyanov⁴¹
A.Straessner²⁰ K.Sudhakar⁹ G.Sultanov⁴¹ L.Z.Sun²¹ S.Sushkov¹ H.Suter⁴⁶ J.D.Swain¹⁰ Z.Szillasi^{25,4} X.W.Tang⁷
P.Tarjan¹⁵ L.Tauscher⁵ L.Taylor¹⁰ B.Tellili²³ D.Teyssier²³ C.Timmermans³⁰ Samuel C.C.Ting¹³ S.M.Ting¹³
S.C.Tonwar⁹ J.Tóth¹² C.Tully³⁶ K.L.Tung⁷ J.Ulbricht⁴⁶ E.Valente³⁸ R.T.Van de Walle³⁰ R.Vasquez⁴³
V.Veszpremi²⁵ G.Vesztergombi¹² I.Vetlitsky²⁷ D.Vicinanza³⁹ G.Viertel⁴⁶ S.Villa³⁷ M.Vivargent⁴ S.Vlachos⁵
I.Vodopianov²⁵ H.Vogel³⁴ H.Vogt⁴⁵ I.Vorobiev^{34,27} A.A.Vorobyov³³ M.Wadhwa⁵ Q.Wang³⁰ X.L.Wang²¹
Z.M.Wang²¹ M.Weber¹ P.Wienemann¹ H.Wilkens³⁰ S.Wynhoff³⁶ L.Xia³¹ Z.Z.Xu²¹ J.Yamamoto³ B.Z.Yang²¹
C.G.Yang⁷ H.J.Yang³ M.Yang⁷ S.C.Yeh⁴⁹ An.Zalite³³ Yu.Zalite³³ Z.P.Zhang²¹ J.Zhao²¹ G.Y.Zhu⁷ R.Y.Zhu³¹
H.L.Zhuang⁷ A.Zichichi^{8,18,19} B.Zimmermann⁴⁶ M.Zöller¹

- 1 III. Physikalisches Institut, RWTH, D-52056 Aachen, Germany[§]
 - 2 National Institute for High Energy Physics, NIKHEF, and University of Amsterdam, NL-1009 DB Amsterdam, The Netherlands
 - 3 University of Michigan, Ann Arbor, MI 48109, USA
 - 4 Laboratoire d'Annecy-le-Vieux de Physique des Particules, LAPP,IN2P3-CNRS, BP 110, F-74941 Annecy-le-Vieux CEDEX, France
 - 5 Institute of Physics, University of Basel, CH-4056 Basel, Switzerland
 - 6 Louisiana State University, Baton Rouge, LA 70803, USA
 - 7 Institute of High Energy Physics, IHEP, 100039 Beijing, China[△]
 - 8 University of Bologna and INFN-Sezione di Bologna, I-40126 Bologna, Italy
 - 9 Tata Institute of Fundamental Research, Mumbai (Bombay) 400 005, India
 - 10 Northeastern University, Boston, MA 02115, USA
 - 11 Institute of Atomic Physics and University of Bucharest, R-76900 Bucharest, Romania
 - 12 Central Research Institute for Physics of the Hungarian Academy of Sciences, H-1525 Budapest 114, Hungary[‡]
 - 13 Massachusetts Institute of Technology, Cambridge, MA 02139, USA
 - 14 Panjab University, Chandigarh 160 014, India.
 - 15 KLTE-ATOMKI, H-4010 Debrecen, Hungary[¶]
 - 16 Department of Experimental Physics, University College Dublin, Belfield, Dublin 4, Ireland
 - 17 INFN Sezione di Firenze and University of Florence, I-50125 Florence, Italy
 - 18 European Laboratory for Particle Physics, CERN, CH-1211 Geneva 23, Switzerland
 - 19 World Laboratory, FBLJA Project, CH-1211 Geneva 23, Switzerland
 - 20 University of Geneva, CH-1211 Geneva 4, Switzerland
 - 21 Chinese University of Science and Technology, USTC, Hefei, Anhui 230 029, China[△]
 - 22 University of Lausanne, CH-1015 Lausanne, Switzerland
 - 23 Institut de Physique Nucléaire de Lyon, IN2P3-CNRS, Université Claude Bernard, F-69622 Villeurbanne, France
 - 24 Centro de Investigaciones Energéticas, Medioambientales y Tecnológicas, CIEMAT, E-28040 Madrid, Spain^b
 - 25 Florida Institute of Technology, Melbourne, FL 32901, USA
 - 26 INFN-Sezione di Milano, I-20133 Milan, Italy
 - 27 Institute of Theoretical and Experimental Physics, ITEP, Moscow, Russia
 - 28 INFN-Sezione di Napoli and University of Naples, I-80125 Naples, Italy
 - 29 Department of Physics, University of Cyprus, Nicosia, Cyprus
 - 30 University of Nijmegen and NIKHEF, NL-6525 ED Nijmegen, The Netherlands
 - 31 California Institute of Technology, Pasadena, CA 91125, USA
 - 32 INFN-Sezione di Perugia and Università Degli Studi di Perugia, I-06100 Perugia, Italy
 - 33 Nuclear Physics Institute, St. Petersburg, Russia
 - 34 Carnegie Mellon University, Pittsburgh, PA 15213, USA
 - 35 INFN-Sezione di Napoli and University of Potenza, I-85100 Potenza, Italy
 - 36 Princeton University, Princeton, NJ 08544, USA
 - 37 University of California, Riverside, CA 92521, USA
 - 38 INFN-Sezione di Roma and University of Rome, "La Sapienza", I-00185 Rome, Italy
 - 39 University and INFN, Salerno, I-84100 Salerno, Italy
 - 40 University of California, San Diego, CA 92093, USA
 - 41 Bulgarian Academy of Sciences, Central Lab. of Mechatronics and Instrumentation, BU-1113 Sofia, Bulgaria
 - 42 The Center for High Energy Physics, Kyungpook National University, 702-701 Taegu, Republic of Korea
 - 43 Purdue University, West Lafayette, IN 47907, USA
 - 44 Paul Scherrer Institut, PSI, CH-5232 Villigen, Switzerland
 - 45 DESY, D-15738 Zeuthen, Germany
 - 46 Eidgenössische Technische Hochschule, ETH Zürich, CH-8093 Zürich, Switzerland
 - 47 University of Hamburg, D-22761 Hamburg, Germany
 - 48 National Central University, Chung-Li, Taiwan, China
 - 49 Department of Physics, National Tsing Hua University, Taiwan, China
- § Supported by the German Bundesministerium für Bildung, Wissenschaft, Forschung und Technologie
- ‡ Supported by the Hungarian OTKA fund under contract numbers T019181, F023259 and T037350.
- ¶ Also supported by the Hungarian OTKA fund under contract number T026178.
- ^b Supported also by the Comisión Interministerial de Ciencia y Tecnología.
- [‡] Also supported by CONICET and Universidad Nacional de La Plata, CC 67, 1900 La Plata, Argentina.
- △ Supported by the National Natural Science Foundation of China.

\sqrt{s} (GeV)	188.6	191.6	195.5	199.5	201.7	205.0	206.6
Luminosity (pb ⁻¹)	176.8	29.8	84.1	84.0	39.2	80.0	130.2

Table 1: Average centre-of-mass energies and corresponding integrated luminosities.

Coupling	$H^{++}H^{--} \rightarrow$	Analyses
h_{ee}	$e^+e^+e^-e^-$	eeee, eee γ
$h_{e\mu}$	$e^+\mu^+e^-\mu^-$	ee $\mu\mu$, e $\gamma\mu\mu$
$h_{e\tau}$	$e^+\tau^+e^-\tau^-$	ee $\tau\tau$, eejetjet, e γ jetjet
$h_{\mu\mu}$	$\mu^+\mu^+\mu^-\mu^-$	$\mu\mu\mu\mu$, $\mu\mu\mu$ MIP
$h_{\mu\tau}$	$\mu^+\tau^+\mu^-\tau^-$	$\mu\mu$ jetjet, $\mu\mu\tau\tau$
$h_{\tau\tau}$	$\tau^+\tau^+\tau^-\tau^-$	ee $\tau\tau$, eejetjet, e γ jetjet, $\mu\mu$ jetjet, $\mu\mu\tau\tau$, $\tau\tau\tau\tau$

Table 2: Analyses used for the different couplings and the corresponding final states.

Coupling	Preselection			Final results			
	N_D	N_B	N_S	N_D	N_B	N_S	ε (%)
h_{ee}	7	10.9	18.3	0	2.7	16.9	46 – 63
$h_{e\mu}$	12	10.2	12.9	9	6.5	12.4	35 – 44
$h_{e\tau}$	1308	1250	7.5	23	21.9	6.5	39 – 44
$h_{\mu\mu}$	0	1.0	10.6	0	0.7	9.2	28 – 32
$h_{\mu\tau}$	8	4.4	8.2	3	4.3	4.7	19 – 22
$h_{\tau\tau}$	1318	1258	12.5	28	27.1	11.1	46 – 53

Table 3: Numbers of events observed in data, N_D , expected from Standard Model processes, N_B , and for a $m_H = 95$ GeV signal, N_S , after the application of the preselection and final selection cuts. Final selection efficiencies, ε , for $m_H = 60 - 100$ GeV are also given.

Coupling	Signal (%)	Background (%)
h_{ee}	1.8	16.8
$h_{e\mu}$	1.8	14.5
$h_{e\tau}$	1.8	9.3
$h_{\mu\mu}$	1.8	15.1
$h_{\mu\tau}$	1.4	10.7
$h_{\tau\tau}$	3.2	10.4

Table 4: Systematic uncertainties on the signal efficiencies and on the background levels for the different couplings.

Coupling	Observed (GeV)	Expected (GeV)
h_{ee}	100.2	100.1
$h_{e\mu}$	99.8	99.7
$h_{e\tau}$	97.2	95.5
$h_{\mu\mu}$	99.4	99.1
$h_{\mu\tau}$	95.5	93.8
$h_{\tau\tau}$	97.3	97.6

Table 5: Observed and expected limits on m_H at 95% confidence level.

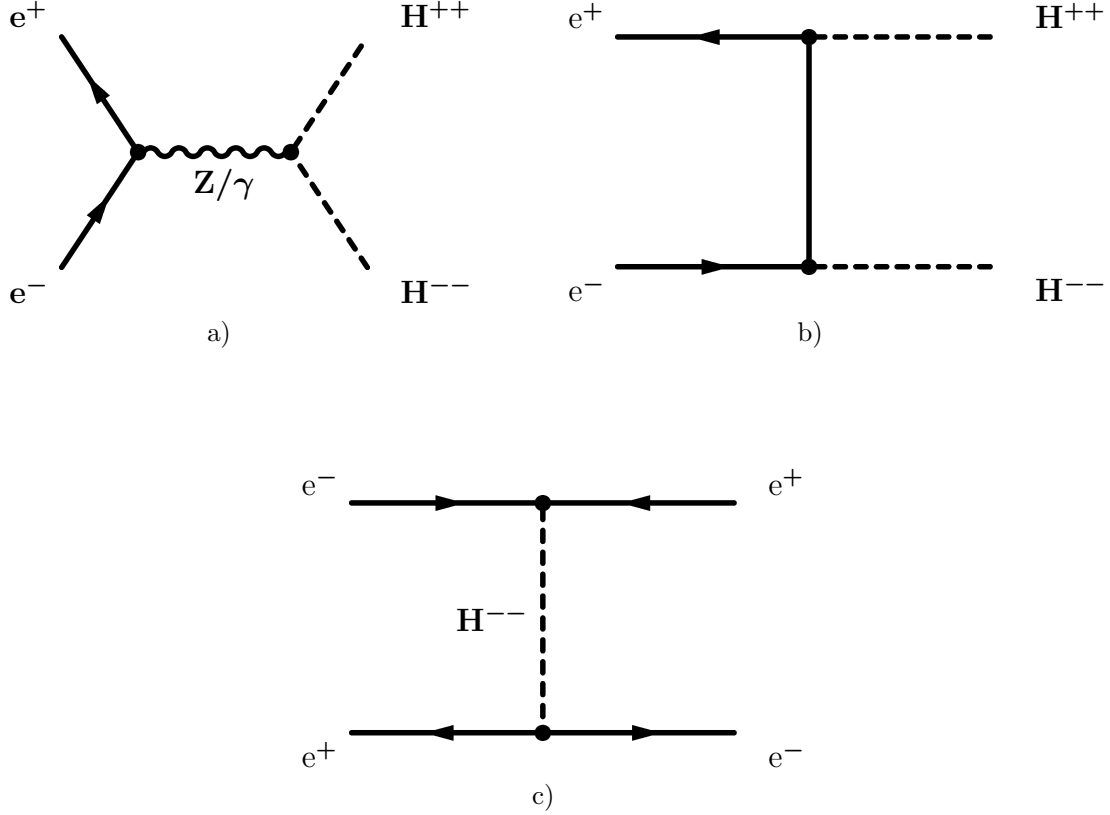


Figure 1: a) s -channel and b) t -channel diagrams for the pair-production of doubly-charged Higgs bosons, c) u -channel doubly-charged Higgs boson exchange in the $e^+e^- \rightarrow e^+e^-$ process.

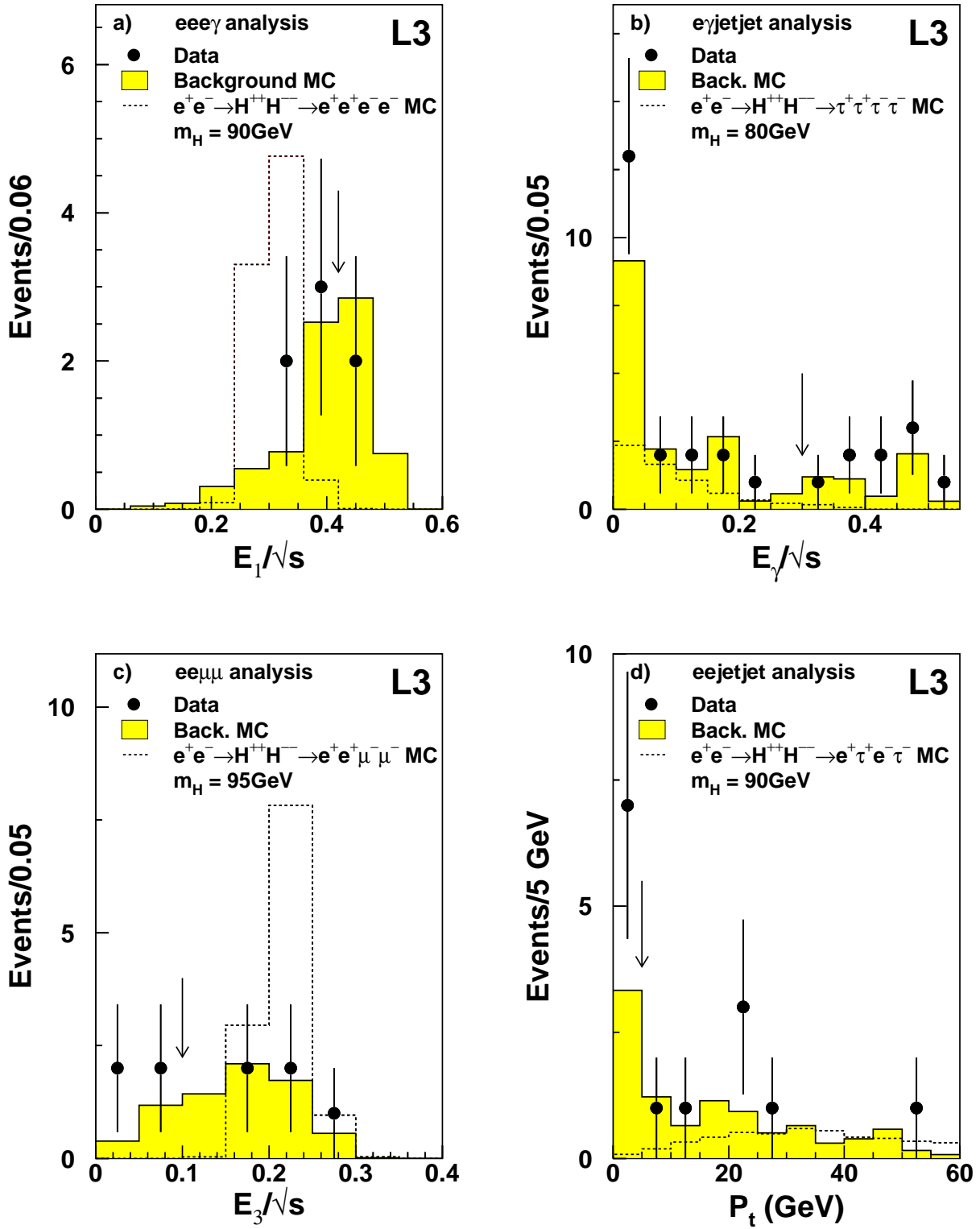


Figure 2: Distributions for data, signal and background Monte Carlo of: a) the energy of the most energetic lepton in the $eee\gamma$ analysis, b) the photon energy for the $e\gamma$ jetjet analysis, c) the energy of the third most energetic lepton for the $ee\mu\mu$ analysis and d) the event transverse momentum for the ee jetjet analysis. The arrows indicate the position of the cuts.

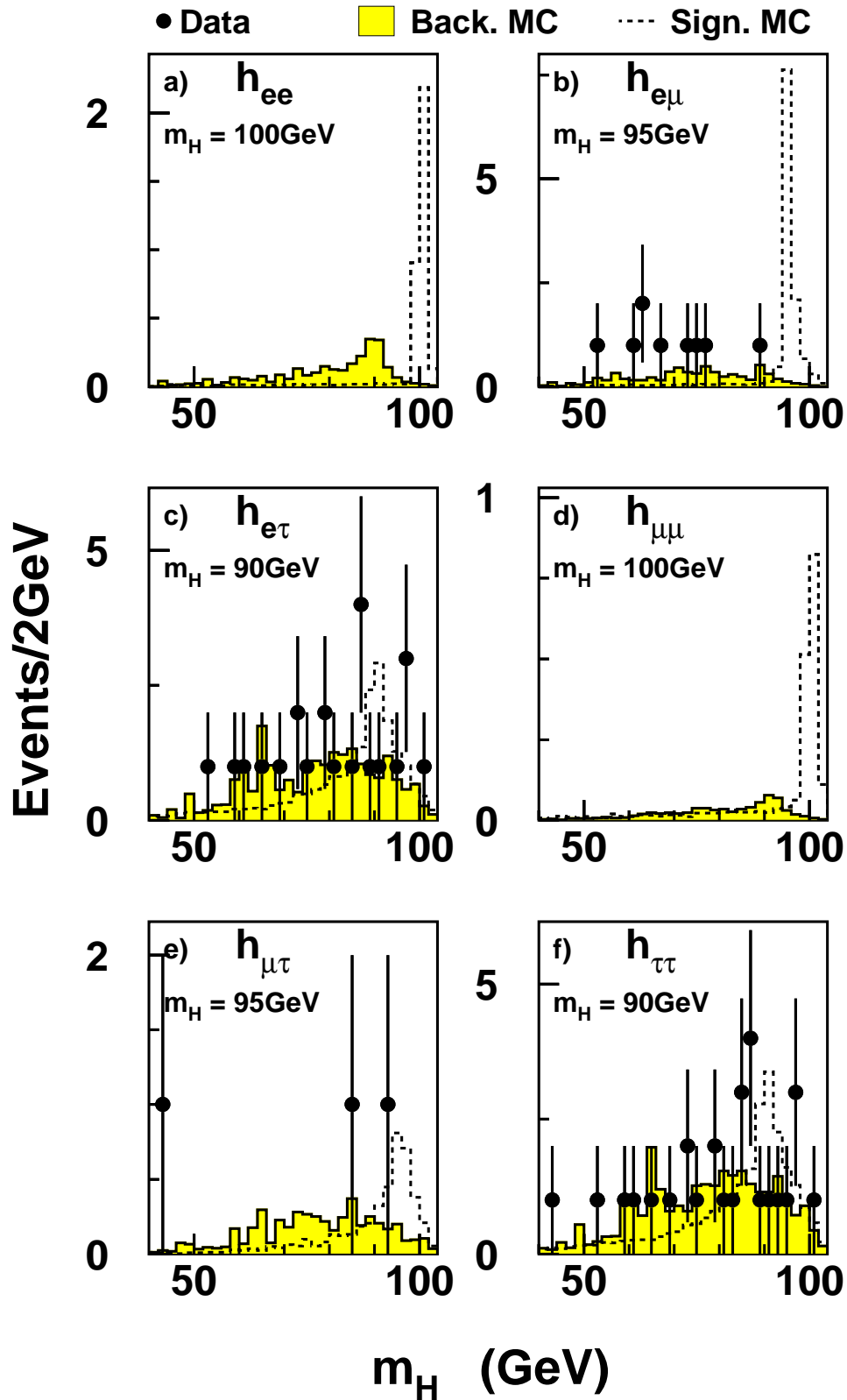


Figure 3: Distributions for data, signal and background Monte Carlo of the reconstructed Higgs mass for the: a) h_{ee} , b) $h_{e\mu}$, c) $h_{e\tau}$, d) $h_{\mu\mu}$, e) $h_{\mu\tau}$ and f) $h_{\tau\tau}$ couplings.

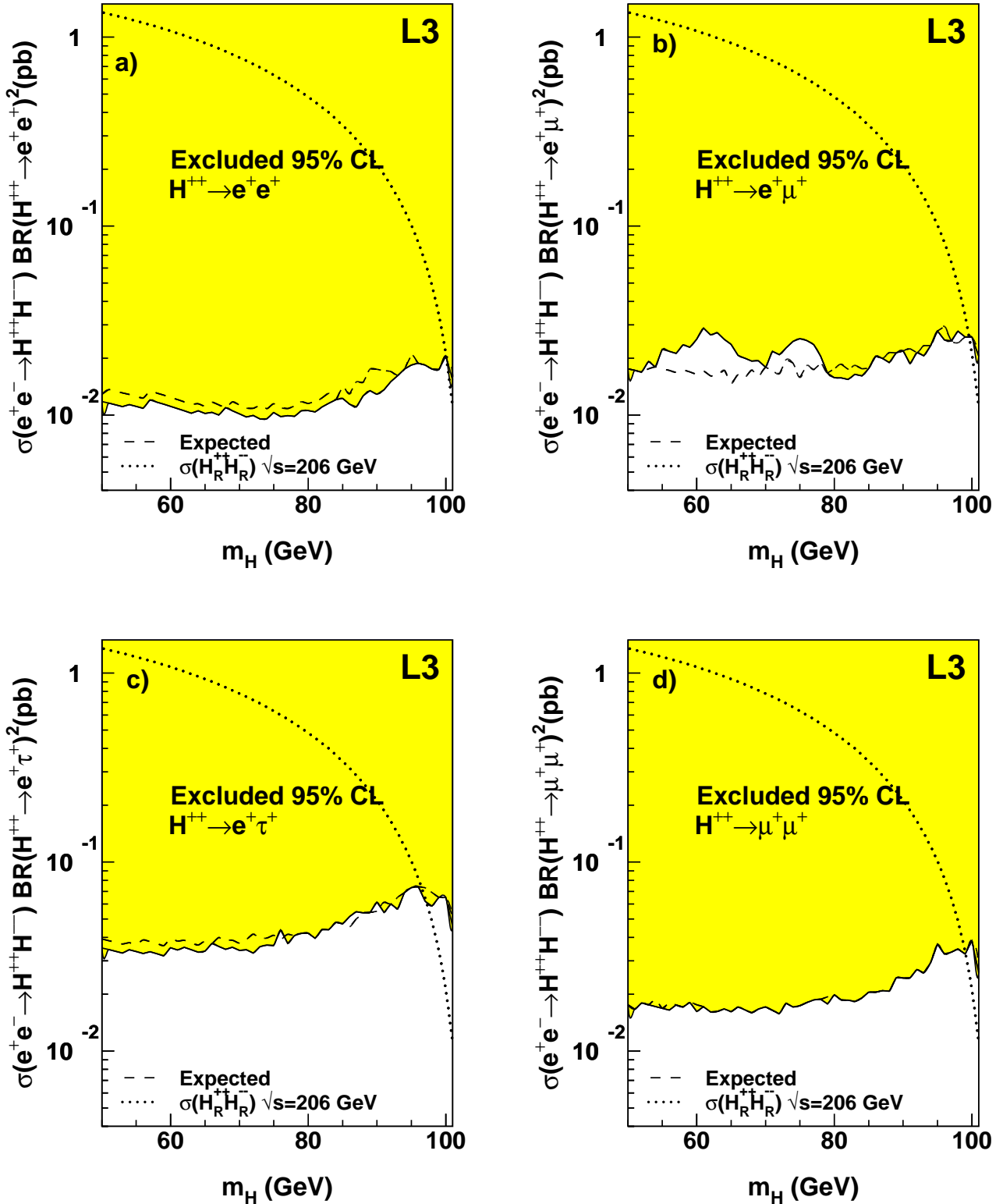


Figure 4: Observed and expected limits on the cross section of doubly charged Higgs boson pair-production times its branching ratio in a given final state as a function of m_H for the: a) h_{ee} , b) $h_{e\mu}$, c) $h_{e\tau}$ and d) $h_{\mu\mu}$ couplings. The expected cross section for the s -channel production of a right-handed doubly-charged Higgs boson is also shown.

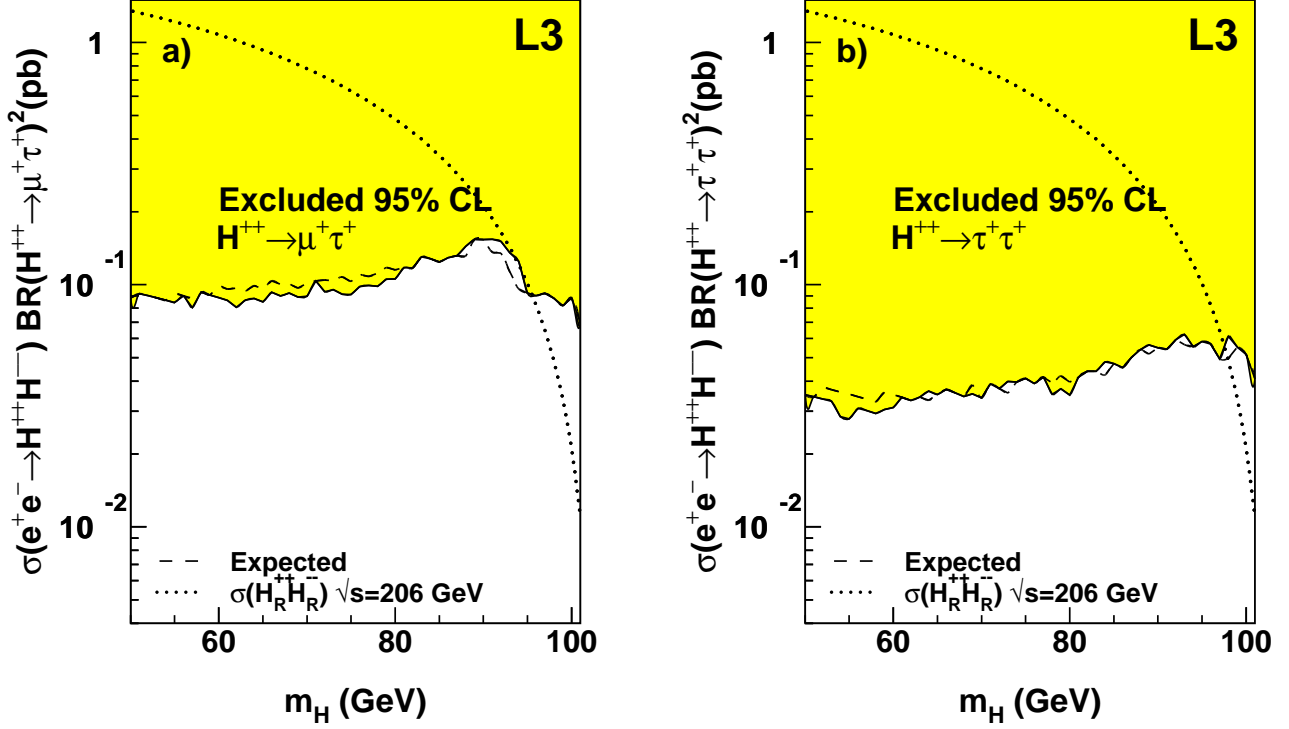


Figure 5: Observed and expected limits on the cross section of doubly charged Higgs boson pair-production times its branching ratio in a given final state as a function of m_H for the: a) $h_{\mu\tau}$ and b) $h_{\tau\tau}$ couplings. The expected cross section for the s -channel production of a right-handed doubly-charged Higgs boson is also shown.

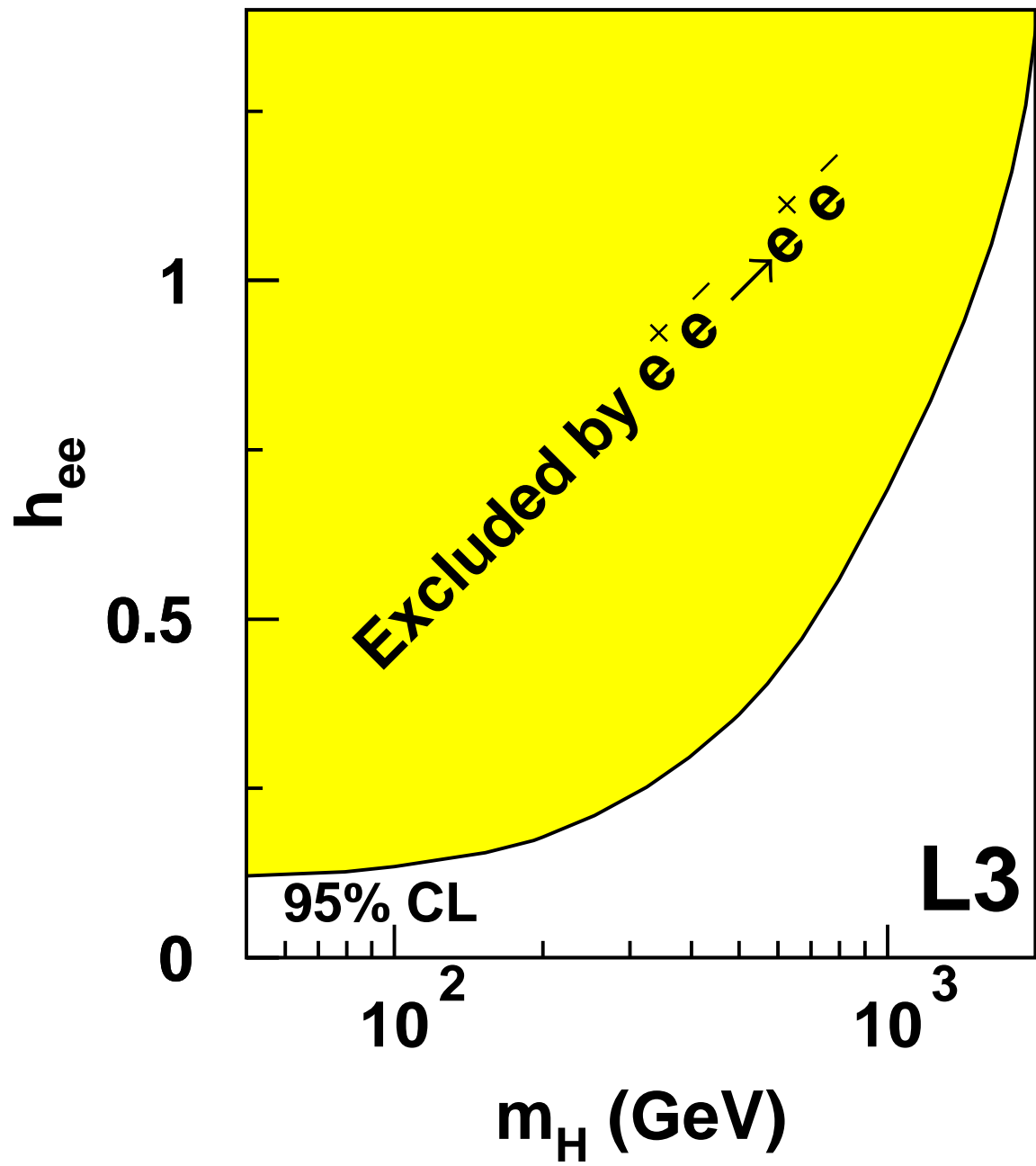


Figure 6: Region in the h_{ee} vs. m_H plane excluded by the study of the $e^+e^- \rightarrow e^+e^-$ process.